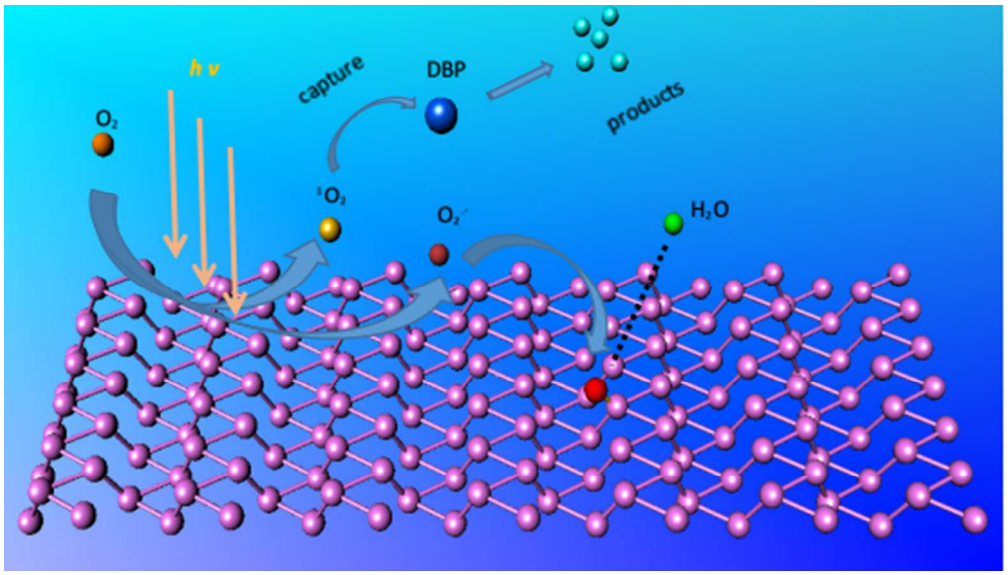

146x82mm (96 x 96 DPI)

Exfoliation of two-dimensional phosphorene sheets with enhanced photocatalytic activity under simulated sunlight

Shuihong Pan,[†] Jun He,[‡] Chengjun Wang [†]* and Yuegang Zuo [§]

[†] College of Chemistry and Materials Engineering

Wenzhou University, Wenzhou 325035, China

[‡] Department of Chemical and Environmental Engineering

The University of Nottingham Ningbo China, Ningbo 315100, China

[§] Department of Chemistry and Biochemistry

University of Massachusetts Dartmouth, North Dartmouth, MA 02747, USA

*Corresponding author

Email: cjwang@wzu.edu.cn

Phone: (+86)15167765923, Fax: (+86) 577-86689300

ORCID: 0000-0001-8433-3512

Submitted to *Environmental Science & Technology Letters*

June 28, 2017

ABSTRACT

The photodegradation of dibutyl phthalate (DBP) over two-dimensional black phosphorene (2D-BP) nanosheets, which were prepared by an environmental friendly solution exfoliation process, in water was investigated under simulated-sunlight. When coexist with water, oxygen, and light, 2D-BP nanosheets can generate the ROS species of $^1O_2$ and $O_2^{\cdot -}$ by energy transfer or charge transfer from excited P* to ground state of oxygen, respectively. The ROS species generation is oxygen dependent and positive related with the amount of 2D-BP added. Results from this study demonstrated that the photodegradation of DBP effectively accelerated via $^1O_2$ oxidation reaction and effects of $O_2^{\cdot -}$ were negligable due to its relative low oxidative reactivity. The present study provides an excellent method for the removal of DBP phthalate from aqueous solution, which might also be applicable to other photodegradable and water soluble organic pollutants.

INTRODUCTION

Phthalate acid esters (PAEs), synthetic organic compounds mainly used as plasticizers for many industrial production, are a class of ubiquitous water contaminants.[1-3] As PAEs are linked together with polymeric materials by Van der Waals force and hydrogen bond rather than chemical bond, they are easy to migrate into the environment during manufacture, use and disposal.[4-5] Owing to the significant hazards to the environment and the organism, some of the PAEs are considered as 'priority pollutants' by the United states Environmental Protection Agency,[1, 6] Dibutyl phthalate (DBP), as a potential endocrine disrupting compound, is one of the most common short-chained phthalate esters, which has been frequently identified in natural environmental water.[7] Given that these pollutants are significantly toxic with potential teratogenicity and carcinogenicity, an effective approach which can be applied to remove these toxic contaminants from natural water is urgently needed.

Reactive oxygen species (ROS) could be produced by many photosensitizers under light illumination, playing a key role in the degradation of organic contaminants.[8-10] Generally speaking, ROS refers to the substance which not only contains oxygen atoms but also possesses active characteristics mainly including of singlet oxygen ($^1O_2$), hydroxyl radicals (·OH), and superoxide radicals ($O_2^{\cdot-}$). Owing to its strong oxidizing properties, ROS achieves the rapid degradation of toxic organic compounds through deep oxidation.[9] Among the ROS, the ·OH is a powerful oxidizing agent and could rapidly and non-selectively damage virtually all types of organic contaminants.[11] Compared with $^1O_2$ and ·OH, $O_2^{\cdot-}$ does not have strong oxidation ability while it has important implications for degrading toxic pollutants. In the past few years, many ROS generating materials have been explored such as various noble metals and metal-free materials including graphene and silicon; however, to the best of our knowledge, apart from their

low water solubility and quantum yield, the above mentioned materials are greatly challenged due to the lack of broad light absorption and poor biocompatibility.[12] Thus, it is highly desirable to seek a new material preferably with high capability to produce ROS under the irradiation of sunlight with long wavelength absorption and exceptional biocompatibility.

Black phosphorus (BP) has attracted scientific attention as a metal-free layered semiconductor because of its unique optical properties and electric structure.[13-16] Composed of puckered layers of phosphorus by weak van der Waals interlayer interaction, BP can be exfoliated from a bulk crystal into mono or few-layer BP nanosheets.[17-18] Compared with other two-dimensional (2D) materials, such as graphene and transition metal dichalcongenides (TMDs), of which the former notoriously has a zero band gap while the latter exhibits an indirect to direct band gap transition from bulk crystals to monolayer sheet, BP possesses a universally tunable direct band gap from 0.3ev for the bulk to 2.0ev for the monolayer.[19] In addition, few-layer BP nanosheets has attractive electronic structure and properties, implying that they would have high potential in photocatalytic application. The previous literature have reported that the ultrathin BP nanosheets could be efficient metal-free semiconductor photosensitizers for the generation of $^1O_2$ and have exceptional biocompatibility.[12, 20] As a result of its broad working spectrum, the few-layer BP nanosheets is considered a superior photosensitizer candidate in accelerating photodegradation of pollutants.

Herein, in the present study, our aims were to prepare and characterize the mono and few-layer 2D-BP nanosheets, to evaluate the performance and investigate the mechanism of the DBP photodegradation over as-prepared 2D-BP nanosheets in water solution under simulated sunlight. The photo-decomposition of organic pollutants with 2D-BP nanosheets investigated in this study could become an attractive technique as promising candidate for water purification process.

MATERIALS AND METHODS

Except acetonitrile and methanol were chromatographic grade, all chemicals used in this study were analytical grade and were sued as received. De-ionized water was used throughout the experiments. Chemical manufactures and reagents preparation are provided in **Text S1**. The solution with dispersion of 2D phosphorene nanosheets were prepared by sonication assisted liquid-phase exfoliation in ice water bath as presented in **Figure 1**. In details, 18 mL of deionized water was added into a 100-mL beaker and covered with parafilm. And the water was bubbled with high-purity nitrogen for 10 min to eliminate the dissolved oxygen to minimize/prevent the oxidation of BP. Then 2.0 mg of the commercially available BP crystal powder was added to the deionized water and immediately sealed followed by sonication (AS20500BT, Atuomatic Science Instrument Co. Ltd., China) in ice water bath for 2 hours. The ice was mainly used to keep the temperature of solution stable during sonication. The beaker was frequently shaken to enhance the effectiveness of exfoliation and dispersion of BP crystal powders in water. Finally, the prepared suspension containing homogeneous 2D phosphorene nanosheets was kept in refrigerator until use. The morphology of BP before and after exfoliation was examined by scanning electron microscope (FEI, Nova NanoSEM 200, USA). The structural characteristics of pristine bulk BP and the BP nanosheets were investigated by Raman microspectrometer (Renishaw, RM-1000, UK) at laser excitation wavelength of 532 nm. The UV-vis absorbance spectrophotometry of the phosphorene nanosheets was investigated by UV spectrophotometer (Shimadzu, UV-1800, Japan).

The DBP sample solutions for photolysis experiments were freshly prepared at concentrations of 30 μg/mL by diluting the DBP stock standard solutions in water. The effects of BP nanosheets on DBP photodegradation were evaluated by spiking DBP standard solutions into

the BP nanosheets suspention containing different concentrations of BP before photolysis experiments. A merry-go-round photochemical chamber reactor equipped with a 500 W Xenon Lamp (290 - 800 nm; Bi-Lang instrument Co., Ltd, Shanghai, China) was used for all photolysis experiments. All laboratory experiments were conducted under the same irradiation intensity. Eight quartz photolysis tubes (40 mm i.d., containing 50 mL of solution) were held in the ring of the merry-go-round accessory. The ring rotated within the reactor chamber at a speed 20 *rpm* to give a uniform irradiation to the photolysis tubes. A hollow cylindrical lampshade with circulated cooling water (the temperature was maintained at 25 °C) was employed to cool the light bulbs. Tubes for the dark control samples were wrapped in aluminum foil. Aliquots of samples (100 μL) were withdrawn at intervals of 1, 2, 4, 6 and 8 hrs and directly injected into high performance liquid chromatography (HPLC) to analyze the concentration of DBP (The HPLC analytical methods are provided in **Text S2**). All experiments were run in duplicate.

RESULTS AND DISCUSSION

Characterization of prepared 2D-BP nanosheets.

The morphologies of BP before and after exfoliation were examined by scanning electron microscope (SEM). The layered structure of primitive bulk BP is clearly observed **(Figure 2a)**. The SEM image of the exfoliated BP nanosheets **(Figure 2b)** indicates that the structure of ultra-thin mono and few-layer 2D-BP nanosheets was formed by the water exfoliation technology with the assistant of sonication. The structural characteristics of pristine bulk BP and the as-prepared ultra-thin 2D-BP nanosheets were investigated by Raman spectroscopy. As presented in **Figure 2c**, the Raman spectra of BP featured three characteristic peaks located at about 360, 437, and 465 cm^{-1}, which are marked as A_g^1, B_{2g}, and A_g^2 modes of BP, respectively.[23, 24] Interestingly, the Raman spectra of BP before and after exfoliation showed nearly identical characteristic peaks,

illustrating the as-obtained 2D-BP nanosheets still maintained the crystal structure of pristine samples. Compared with pristine bulk BP, the central frequency of A_g^2 modes in 2D-BP nanosheets with obvious redshift is noted, while the shift of A_g^1 peak was not significant. In addition, the intensity ratio A_g^1/A_g^2 in 2D-BP nanosheets increased greatly as compared to that in bulk BP. According to previous work on exfoliated BP reported by Favron et al, it is known that the central frequency of A_g^2 modes is most sensitive to changes in the number of layers and the A_g^1 modes change is least significant as the thickness of layers is reduced.[21] Consequently, A_g^2 modes with significant shift was observed. Hence, the successful preparation of mono and few-layer 2D-BP nanosheets in this study could be confirmed by the Ramam spectra.

The as-obtained 2D-BP nanosheets was further examed by UV-vis spectrophotometry to determine their unique optical absorption properties. As presented in **Figure 2d**, the UV-vis optical absorption spectra is consistent with the previous theoretical prediction that the absorption of BP nanosheets is thickness dependent and their direct tunable band gap covers a broad region ranging from 0.3 ev in the pristine bulk samples to 2.0 ev in the single layer phosphorene.[15, 19, 23] It is crucial for 2D-BP nanosheets to be effective photosensitizers to possess an exceptional optical absorption properties.

Accelerated photodegradation of DBP over 2D-BP nanosheets.

To evaluate the performance of 2D-BP nanosheets on photodegradation of DBP in aqueous solution, the degradation efficiency of DBP containing suspended ultra-thin 2D-BP nanosheets was carried out under the irradiation of xenon lamp. Specifically, the purchased bulk BP (1mg or 2mg) was added to an anaerobic deionized water (19.4 mL) that had been bubbled with nitrogen for 10 min to eliminate the dissolved oxygen, and immediately sealed to prevent the solution from air. Afterwards, the mixture was

ultrasonicated in ice water for 2 hours and its color gradually changed from clear to the dark brown as the BP was exfoliated (**Figure S1**). Then, 0.6 mL of DBP (0.1 mg/mL) was added to the sample solution containing suspended ultra-thin 2D-BP nanosheets and placed in the photo-reactor to conduct photodegradation tests. For comparison, the aqueous DBP solution with bulk BP and without BP nanosheets was also tested under the same conditions. As illustrated in **Figure 3a**, after 6 h irradiation, more than 45% of total DBP was degraded in samples containing 2 mg of 2D-BP nanosheets while only 22% DBP was decomposed without BP nanosheets. The photodegradation efficiency of DBP gradually increased with the increase of BP quantity added (0, 1.0 and 2.0 mg), indicating that the photodegradation of DBP was notably accelerated due to the presence of 2D-BP nanosheets.

Given the exceptional absorption window from UV-Vis to near-infrared region and unique electron accepting abilities, BP nanosheets could be excited under sunlight irradiation and further generate ROS species which may be beneficial to the degradation of organic compounds when water, oxygen and visible light are simultaneously present.[21-22, 25] To evaluate the possible involvement of the ROS for the photodegradation of DBP in the presence of BP nanosheets, the quenching experiments for reactive oxygen species including ·OH, $^1O_2$ and $O_2^{\bullet -}$ were conducted (**Text S3**). As displayed in **Figure 3b**, the degradation of DBP was significantly inhibited by adding DABCO, indicating that 2D-BP nanosheets do generate the $^1O_2$, which is a dominant oxidizing agent and significantly accelerates the photodegradation of DBP through deep oxidation. After adding a quantitative amount of IPA and NBT as scavengers of ·OH and $O_2^{\bullet -}$, the removal efficiency of DBP showed negligible change (**Figure 3b**), further indicating the active

species generated by BP is singlet oxygen $^1O_2$ under light irradiation. However, the UV-Vis absorption of NBT gradually decay with the light irradiation during the photolysis process (**Figure S2)**, implying the generation of $O_2^{\cdot -}$ consuming more NBT over time. Therefore, the negligible contribution to the DBP degradation by $O_2^{\cdot -}$ due to its weak oxidizing properties compared to $^1O_2$. Furthermore, to exclude the possible direct reaction between DBP and photoexcited BP nanosheets, the photolysis of DBP was carried out under continuous N_2 and O_2 purge, respectively. The removl efficiency of DBP decreased under N_2 conditions, while dramatically increased under O_2 conditions. The oxygen content dependent character clearly indicates that the $^1O_2$ is generated under photosensitizing process by energy transfer from BP to ground-state oxygen. Although both the ultrathin 2D-BP nanosheets and bulk BP can induce the formation of $^1O_2$, the DBP decomposition efficiency in the case of ultrathin 2D-BP nanosheets is significantly higher than that of corresponding bulk (**Figure 3a**). The dramatic enhancement of the $^1O_2$ generation would attribute to the ultrathin character of the nanosheets, which not only provides rich surface atoms serving as the active sites but also reduces the electron-hole recombination rate. Besides, the much higher charge-carried mobility of the ultrathin BP nanosheets toward that of corresponding bulk sample would also benefit for the $^1O_2$ generation.

Overall, the generation of ROS species over 2D-BP nanosheets and accelerated photodegradation mechanism of DBP when water, oxygen, 2D-BP nanosheets and light coexist are proposed as follows:

$$P + h\upsilon \rightarrow P^* \quad (1)$$

$$P^* + O_2 \rightarrow {}^1O_2 + P \quad (2)$$

$$P^* + O_2 \rightarrow O_2 \cdot^- + P \quad (3)$$

$$^1O_2 + DBP \rightarrow \text{degraded products} \quad (4)$$

Firstly, the electrons (e^-) on phosphorous are excited across the direct band gap to the conduction band, creating excited P*; secondly, $^1O_2$ is generated through energy transfer from P* to ground state of O_2 or $O_2 \cdot^-$ is formed through a charge transfer reaction under light; thirdly, DBP is decomposed via $^1O_2$ oxidation. Although the light induced degradation of BP may affect its photocatalytic acitivity and need further modification for industry applications, the high photocatalytic reactivity of 2D-BP nanosheets for organic compounds decomposition could become an attractive technique for control of environmental organic pollutants in water.

ACKNOWLEDGMENTS

The research project was jointly supported by the National Natural Science Foundation of China (21477088) and Natural Science Foundation of Zhejiang Province (LY17B070001).

NOTES

The authors declare no competin financial interest.

REFERENCES

(1) Zheng, X. X.; Zhang, B. T.; Teng, Y. G. Distribution of phthalate acid esters in lakes of Beijing and its relationship with anthropogenic activities. *Sci. Total Environ.* **2014**, *476-477,* 107-113.

(2) Barreca, S.; Indelicato, R.; Orecchio, S.; Pace, A. Photodegradation of selected phthalates on mural painting surfaces under UV light irradiation. *Microchem. J.* **2014**, *114,* 192-196.

(3) Chen, Y. H.; Chen, L. L.; Shang, N. C. Photocatalytic degradation of dimethyl phthalate in an aqueous solution with Pt-doped TiO_2-coated magnetic PMMA microspheres. *J. Hazard. Mater.* **2009**, *172,* 20-29.

(4) Peng, X. W.; Li, X. G.; Feng, L. J. Behavior of stable carbon isotope of phthalate acid esters during photolysis under ultraviolet irradiation. *Chemosphere* **2013**, *92,* 1557-1562.

(5) Mailhot, G.; Sarakha, M.; Lavedrine, B.; Cáceres, J.; Malato, S. Fe(III)-solar light induced degradation of diethyl phthalate (DEP) in aqueous solutions. *Chemosphere* **2002**, *49,* 525-532.

(6) Yang, G. P.; Zhao, X. K.; Sun, X. J.; Lu, X. L. Oxidative degradation of diethyl phthalate by photochemically-enhanced Fenton reaction. *J. Hazard. Mater.* **2005**, *126,* 112-118.

(7) Lau, T. K.; Chu, W.; Graham, N. The degradation of endocrine disruptor di-n-butyl phthalate by UV irradiation: A photolysis and product study. *Chemosphere* **2005**, *60,* 1045-1053.

(8) Ciesla, P.; Kocot, P.; Mytych, P.; Stasicka, Z. Homogeneous photocatalysis by transition metal complexes in the environment. *J. Mol. Catal. A: chem.* **2004**, *224,* 17-33.

(9) Li, Y.; Zhang, W.; Niu, J. F.; Chen, Y. S. Mechanism of photogenerated reactive oxygen species and correlation with the antibacterial properties of engineered metal-oxide nanoparticles. *ACS Nano* **2012**, *6,* 5164-5173.

(10) Lee, J.; Fortner, J. D.; Hughes J. B.; Kim, J. H. Photochemical Production of Reactive Oxygen Species by C_{60} in the Aqueous Phase during UV Irradiation. *Environ. Sci. Technol.* **2007**, *41,* 2529-2535.

(11) Zhao, X. K.; Yang, G. P.; Wang, Y. J.; Gao, X. C. Photochemical degradation of dimethyl phthalate by Fenton reagent. *J. Photoch. Photobio. A* **2004**, *161,* 215-220.

(12) Wang, H.; Yang, X. Z.; Shao, W.; Chen, S. C.; Xie, J. F.; Zhang, X. D.; Wang J.; Xie, Y. Ultrathin Black Phosphorus Nanosheets for Efficient Singlet Oxygen Generation. *J. Am. Chem. Soc.* **2015**, *137*, 11376-11382.

(13) Tran, V.; Yang, L. Scaling laws for the band gap and optical response of phosphorene nanoribbons. *Phys. Rev. B* **2014**, *89,* 245407.

(14) Sun, Z. B.; Xie, H. H.; Tang, S. Y.; Yu, X. F.; Guo, Z. N.; Shao, J. D.; Zhang, H.; Huang, H.; Wang, H. Y.; Chu, P. K. Ultrasmall Black Phosphorus Quantum Dots: Synthesis and Use as Photothermal Agents. *Angew. Chem. Int. Ed.* **2015**, *54,* 11526-11530.

(15) Rahman, M. Z.; Kwong, C. W.; Davey, K.; Qiao, S. Z. 2D phosphorene as a water splitting photocatalyst: fundamentals to applications. *Energy Environ. Sci.* **2016**, *9,* 709-728.

(16) Doganov, R. A.; O'Farrell, E. C.T.; Koenig, S. P.; Yeo, Y.; Ziletti, A.; Carvalho, A.; Campbell, D. K.; Coker, D. F.; Watanabe, K. J.; Taniguchi, T. S.; Neto, A. H.; Ozyilmaz, C. B. Transport properties of pristine few-layer black phosphorus by van der Waals passivation in an inert atmosphere. *Nat. Commun.* **2015**, *6,* 6647.

(17) Bagheri, S.; Mansouri,N.; Aghaie, E. Phosphorene: A new competitor for graphene. *Int. J. Hydrogen Energy* **2016**, *41,* 4085-4095.

(18) Lewis, E. A.; Brent, J. R.; Derby, B.; Haigh, S. J.; Lewis, D. J. Solution processing of two-dimensional black phosphorus. *Chem. Commun.* **2017**, *53,* 1445-1458.

(19) Kang, J. H.; Wood, J. D.; Wells, S. A.; Lee, J. H.; Liu, X. L.; Chen, K. S.; Hersam, M. C. Solvent Exfoliation of Electronic-Grade, Two-Dimensional Black Phosphorus. *ACS Nano* **2015**, *9,* 3596-3604.

(20) Chen, W. S.; Yang, J. Q.; Liu, H.; Chen, M.; Zeng, K. J.; Sheng, P.; Liu, Z. J.; Han, Y. J.; Wang, L. Q.; LI, J.; Deng, L.; Liu, Y. N.; Guo, S. J. Black Phosphorus Nanosheet-Based Drug Delivery System for Synergistic Photodynamic/Photothermal/Chemotherapy of Cancer. *Adv. Mater.* **2017,** *29,* 1603864.

(21) Favron, A.; Gaufres, E.; Fossard, F.; Phaneuf-L'Heureux, A-L.; Tang, N. Y-W.; Levesque, P. L.; Loiseau, A.; Leonelli, R.; Francoeur S.; Martel, R. Photooxidation and quantum confinement effects in exfoliated black phosphorus. *Nat. Mater.* **2015**, *14,* 826-832.

(22) Zhou, Q. H.; Chen, Q.; Tong, Y. L.; Wang, J. L. Light-Induced Ambient Degradation of Few-Layer Black Phosphorus: Mechanism and Protection. *Angew. Chem. Int. Ed.* **2016**, *55,* 11437-11441.

(23) Guo, Z.; Zhang, H.; Lu, S. B.; Wang, Z. T.; Tang, S. Y.; Shao, J. D.; Sun, Z. B.; Xie, H. H.; Wang, H. Y.; Yu, X. F.; Chu, P. K. From Black Phosphorus to Phosphorene: Basic Solvent Exfoliation, Evolution of Raman Scattering, and Applications to Ultrafast Photonics. *Adv. Funct. Mater.* **2015**, *25,* 6996-7002.

(24) Xu, J. Y.; Gao, L. F.; Hu, C. X.; Zhu, Z. Y.; Zhao, M.; Wang, Q.; Zhang, H. L. Preparation of large size, few-layer black phosphorus nanosheets via phytic acid-assisted liquid exfoliation. *Chem. Commun.* **2016**, *52,* 8107-8110.

(25) Ziletti, A.; Carvalho, A.; Campbell, D. K.; Coker, D. F.; Neto, A. H. C. Oxygen Defects in Phosphorene. *Phys. Rev. Lett.* **2015**, *114,* 046801.

Figure Captions

Figure 1. Schematic illustration of the fabrication process of water exfoliated 2D-BP nanosheets

Figure 2. Scanning electron microscope (SEM) images of (a) the bulk BP before exfoliation and (b) the exfoliated 2D-BP nanosheets; (c) Raman spectra and (d) UV-vis spectra of BP nanosheets

Figure 3. Photodegradation of DBP in aqueous solutions (a) containing different types and amounts of BP nanosheets; (b) containing 2 mg 2D-BP nanosheets and ROS quenchers

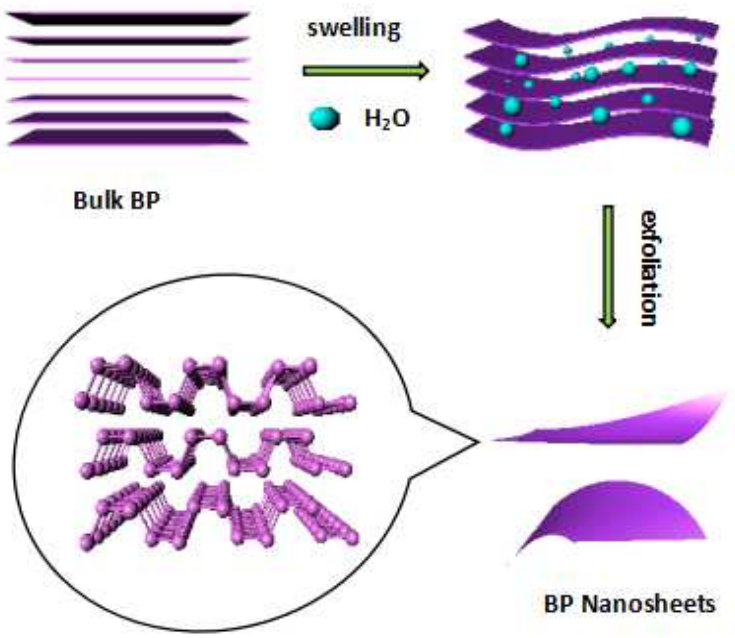

Figure 1. Schematic illustration of the fabrication process of water exfoliated 2D-BP nanosheets.

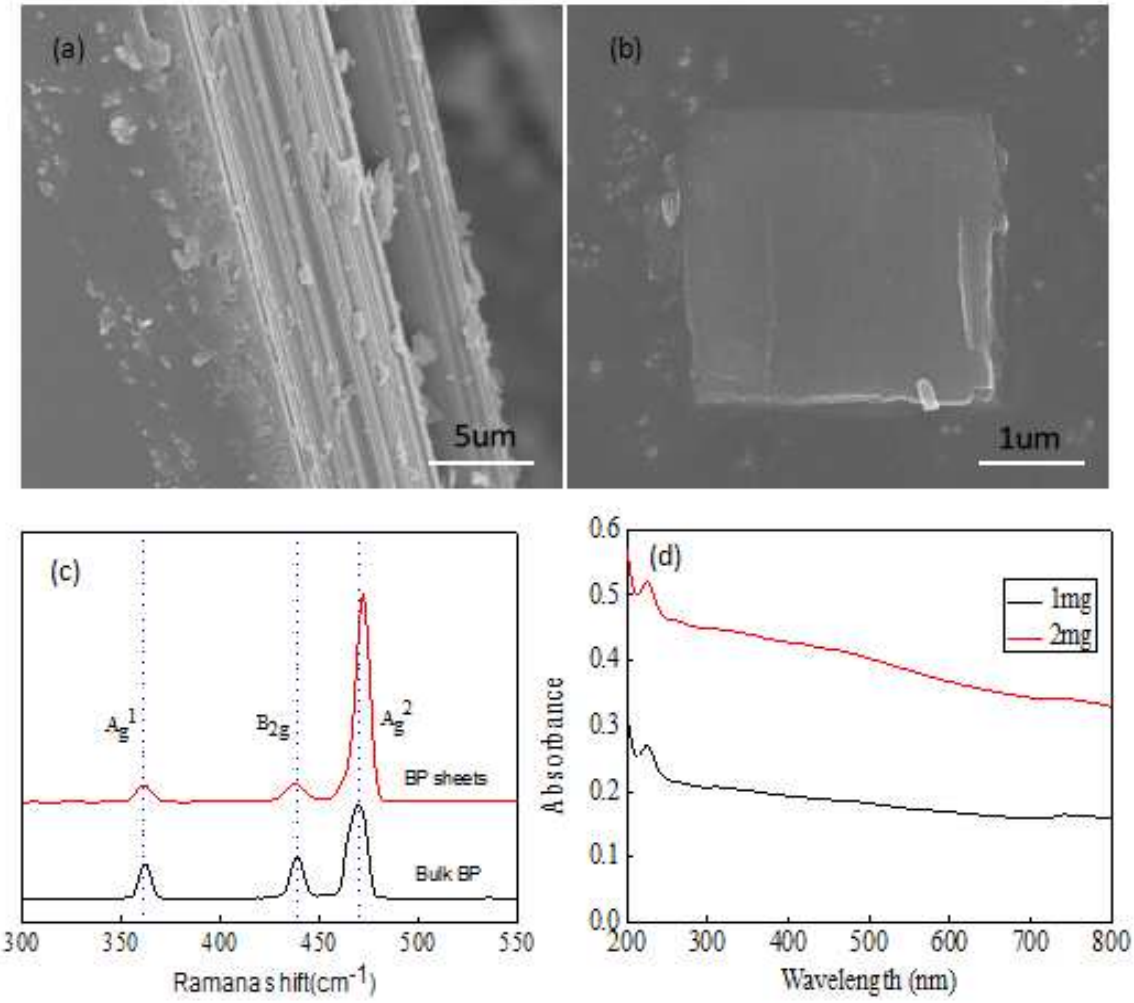

Figure 2. Scanning electron microscope (SEM) images of (a) the bulk BP before exfoliation and (b) the exfoliated BP nanosheets; (c) Raman spectra and (d) UV-vis spectra of BP nanosheets

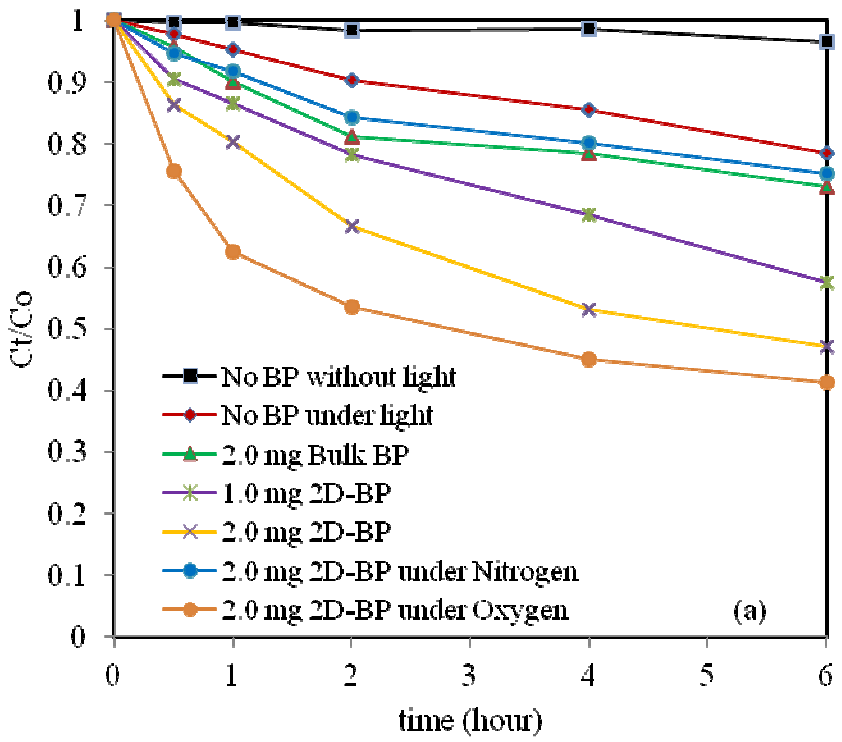

355

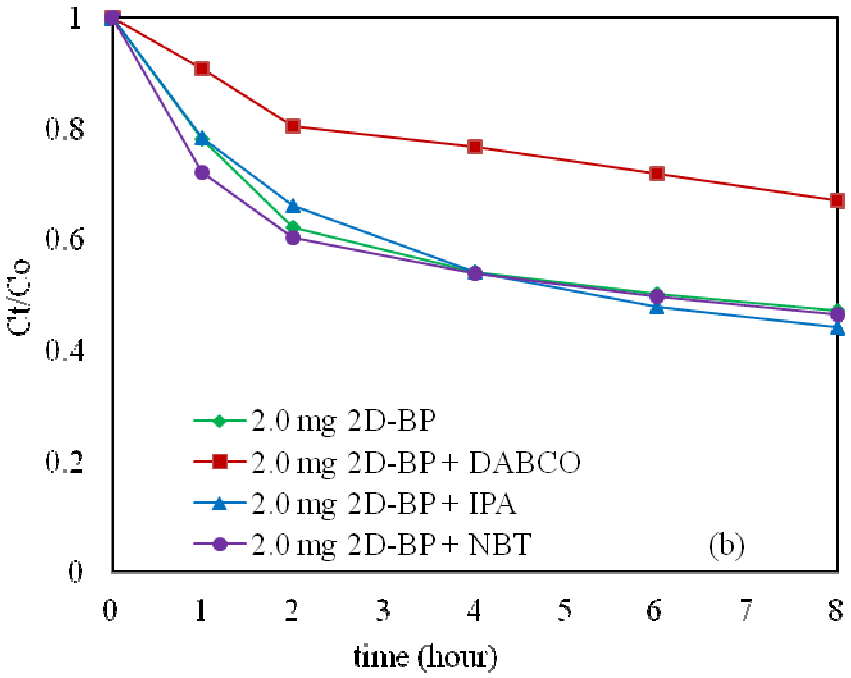

356

357 **Figure 3.** Photodegradation of DBP in aqueous solutions (a) containing different types and

358 amounts of BP nanosheets; (b) containing 2 mg 2D-BP nanosheets and ROS quenchers

359